REPORT DOCUMENTATION PAGE

Form Approved
OMB No. 0704-0188

1. REPORT DATE *(DD-MM-YYYY)*	2. REPORT TYPE	3. DATES COVERED *(From - To)*
	Technical Papers	

4. TITLE AND SUBTITLE	5a. CONTRACT NUMBER
	5b. GRANT NUMBER
	5c. PROGRAM ELEMENT NUMBER
6. AUTHOR(S)	5d. PROJECT NUMBER
	5e. TASK NUMBER
	5f. WORK UNIT NUMBER

7. PERFORMING ORGANIZATION NAME(S) AND ADDRESS(ES)	8. PERFORMING ORGANIZATION REPORT
Air Force Research Laboratory (AFMC) AFRL/PRS 5 Pollux Drive Edwards AFB CA 93524-7048	
9. SPONSORING / MONITORING AGENCY NAME(S) AND ADDRESS(ES)	**10. SPONSOR/MONITOR'S ACRONYM(S)**
Air Force Research Laboratory (AFMC) AFRL/PRS 5 Pollux Drive Edwards AFB CA 93524-7048	**11. SPONSOR/MONITOR'S NUMBER(S)**

12. DISTRIBUTION / AVAILABILITY STATEMENT

Approved for public release; distribution unlimited.

13. SUPPLEMENTARY NOTES

14. ABSTRACT

15. SUBJECT TERMS

16. SECURITY CLASSIFICATION OF:			17. LIMITATION OF ABSTRACT	18. NUMBER OF PAGES	19a. NAME OF RESPONSIBLE PERSON
					Leilani Richardson
a. REPORT	b. ABSTRACT	c. THIS PAGE	A		19b. TELEPHONE NUMBER *(include area code)*
Unclassified	Unclassified	Unclassified			(661) 275-5015

8 separate items enclosed

TP-1998-159

S1

MEMORANDUM FOR IN-HOUSE PUBLICATIONS

13 Jul 98

FROM: PROI (TI) (STINFO)

SUBJECT: Authorization for Release of Technical Information, Control Number: AFRL-PR-ED-TP-1998-159

Greg Spanjers "PPT Research at AFRL: Material Probes to Measure the Magnetic Field Distribution in a Pulsed Plasma Thruster" **AIAA paper** **(Statement A)**

AIAA 98-3659

PPT Research at AFRL: Material Probes to Measure the Magnetic Field Distribution in a Pulsed Plasma Thruster

G. G. Spanjers
USAF Research Laboratory
Edwards AFB, CA

R. A. Spores
USAF Research Laboratory
Edwards AFB, CA

34th AIAA/ASME/SAE/ASEE
Joint Propulsion Conference & Exhibit
July 12 - 15, 1998 / Cleveland, OH

efficiency and a low energy efficiency.[4] Previous AFRL research has concentrated on understanding the sources of the low propellant efficiency. It was found that significant propellant losses are incurred due to late-time vaporization of propellant material after the current pulse has ended,[4] and due to the emission of large particulates of propellant material.[5] AFRL research is presently testing possible methods of ameliorating these propellant losses including controlling the propellant temperature,[6] and modifying the thermal mechanical properties of the propellant.

The focus of the PPT basic research program at AFRL has now shifted to understanding the sources of the low energy efficiency. Based on previous research[7,8] modifications such as changing the electrode geometry, discharge frequency, and discharge energy may all result in moderate increases to the energy efficiency. What is required from a basic research standpoint is a diagnostic capability that can acquire information with sufficient accuracy to enable PPT designers to understand why certain influences increase performance – and then design PPTs which maximize these effects. To model a fluid description of the PPT plasma, the critical measurements are magnetic field and density. Temperature, composition and charge state also become critical as the models become more detailed. This paper describes a magnetic field probe array used at AFRL to map the magnetic fields in a laboratory model PPT. The paper focuses on determining to what extent the probe perturbs the plasma, the measurement limitations. Also discussed are options towards making this critical measurement with increased accuracy.

II. Experimental Apparatus

A. Description of Magnetic Probe Array

Ideally, an array of several probe coil sets, each with three orthogonal windings to simultaneously measure the full magnetic field vector at several locations is desired. In practice, a set of four probe sets requires a cladding diameter of at least 6mm in order to fit the windings, wires and shield into the package. A 6-mm OD cladding is significant compared to the 25.4 mm x 25.4 mm dimension of the PPT propellant face, resulting in an unacceptably low spatial resolution. In addition, tests with 6-mm probe claddings showed that the location of the discharge arc appeared to be affected by the placement of the probe.

To compromise between the requirements for a small diameter package and an array of coil sensors, the probe package is designed with a small cladding diameter within the measurement region and a larger diameter downstream of the thruster. The probe array is shown in Fig. 2 inserted between the electrodes of the AFRL Pulsed Plasma thruster XPPT-1. Only one component of the magnetic field is measured. Each coil is oval in shape, 1.2 mm diameter and 3.5 mm long, and consists of four turns of wire. The array is encased in a 2 mm ID x 3 mm ID quartz tube with the end sealed. The quartz tube is expanded to 4 mm ID x 6 mm OD, 5 cm downstream of the thruster to increase the space available to bring the coil leads and electrostatic shield back through the quartz tube. Two leads are brought back for each coil in a twisted pair for electromagnetic shielding. The leads are encased in a 3.2 mm ID x 4.0 mm OD brass tube that is grounded for electrostatic shielding and provides 14 μS of magnetic shielding. The probe signals are passively integrated with a 20 μS RC integration time and digitally stored in an oscilloscope.

B. Probe Cladding

Subjected to the heat flux from the plasma, the probe cladding can ablate and quickly emit a mass of material much greater than the total mass of the plasma being measured. This can strongly effect the magnetic field distribution and perturb the measurement, although the sensitivity of the plasma to these effects depends on many

parameters. A criterion for a probe to significantly affect the plasma is the time it takes for the surface of the probe to boil, t_B. For sufficiently short times-scales, the heat deposition into the cladding can be considered using a 1-dimensional approximation, ignoring the effects of heat conduction.[9]

$$(1) \quad t_B P^2 = \frac{T_B \pi \kappa \rho C}{4}$$

where P is the power per unit area deposited in the cladding, T_B is the boiling temperature of the material, κ is the thermal conductivity, ρ is the specific gravity, and C is the specific heat. The right-hand-side of the equation is dependent only on the material properties of the cladding. For the directed flux of the PPT discharge, the dominant source of heat is the deposition of the ion kinetic energy. The power density is the kinetic energy per ion times the collision frequency with the probe.

$$(2) \quad P = (\frac{1}{2} m_i v^2) nv$$

The ion mass is estimated as 16.7 times the proton mass, which is the weighted average of the atomic masses of the Teflon™ constituents: carbon and fluorine. Figure 3 shows the contours of constant boil time as a function of the ion density and velocity calculated from Eqns. 1 and 2. Also shown is a region that may be the relevant regime of operation for a 20 J PPT. There is clearly significant uncertainty in the identification of this regime since both the ion density and velocity are difficult to measure. The density is based on interferometer measurements[4] of the line-integrated electron density that showed a peak of 7.5 x 10^{15} cm^{-2}. Assuming all of the ions concentrated in a 3mm wide discharge arc with single ionization, this would imply a local ion density of 2.5 x 10^{16} cm^{-3}. The ion velocity is estimated from reported measurements, generally using time-of-flight diagnostics. The required "belief time" for the probe is approximately 10 μS which is the time for the discharge current to dissipate. Figure 3 indicates that the possibility exists for probe cladding to boil within this time. However, the contours of Fig. 3 are conservative for several reasons:

- It is assumed that the full density and velocity are impinging on the probe for the entire boil time. In practice, these values will vary during the boil time. Assuming a linear rise approximation, using the average values of n/2 and v/2 decreases the power deposition by a factor of 16.
- Probes inserted near the propellant face are not subjected to ions accelerated to their peak velocity.
- All ion collisions with the probe are assumed fully inelastic, depositing al of the kinetic energy into the cladding.

The connection between the two quartz tubes is sealed with Torr-Seal ceramic epoxy. The Torr-Seal is more likely than the quartz to ablate when subjected to the plasma heat flux. Its use here is justified since the probe is designed for use in plasma with a directed velocity. Torr-Seal material heated and ablated by the energetic plasma is behind the region where the magnetic field is measured. Vapor that is emitted can only transport back into the PPT acceleration region at thermal velocities. For a 300 m/s thermal velocity, the Torr-Seal vapor would require 92 μS to transit 2.75 cm upstream to the magnetic field probes, which is an order of magnitude longer than the experimental time-scale.

C. Probe Response Time and Calibration

The probe response time is determined by the inductance of the sensor coils and the load resistance. Using the approximations of Lovberg,[10] the response time is approximately 28 pS. After an experimental run, the probe is observed to have a thin coating deposited by the PPT exhaust that is presumably carbon. Sufficiently

conductive, this coating could slow the response time of the coils to the magnetic field diffusion time through the conductive coating. Assuming carbon resistance for the coating, a resistive diffusion time of 10 nS would require a coating 38-μm thick. If all of the PPT exhaust were to deposit on the probe, this is equivalent to the mass expelled by the PPT in 54,000 discharges which is an order-of-magnitude longer than the experimental runs considered in the present work. Thus, the coating is not expected to affect the probe response time. Any effects it may have on the cladding ablation are unknown.

The probe is calibrated using a pulsed discharge through a 12.7-cm wide, 12.7-cm long, 2.54-cm thick aluminum strip-line. The current is discharged in the strip-line with a period of 8 μS, approximately equal to the PPT discharge period. The strip-line dimensions are clearly too small to preclude systematic errors due to fringing fields. To account for these effects, the strip-line magnetic fields were mapped out independent of the probe calibration.

III. Experimental Measurements

The experiments are performed at the Air Force Research Laboratory in Chamber 5 of the Electric Propulsion Laboratory. Chamber 5 is 1.2 m in diameter and 1.8 m in length. Typical base pressures of 3×10^{-5} Torr are achieved using two 1400-l/s turbomolecular pumps. The experiments are conducted using XPPT-1 (Experimental Pulsed Plasma Thruster #1).[4] The XPPT-1 is similar to the LES 8/9 PPT electrically and geometrically, however diagnostic access has been increased in the XPPT-1 design by removing the housing around the electrodes. All measurements are collected using a 20-J discharge with a 1-Hz discharge rate. The thruster is allowed to complete 5000 discharges before acquiring data to allow thruster transient effects to dissipate.

The probe array is moved using translation stages controlled with manual rotary vacuum feedthroughs. The PPT continues to fire during times when the probe is being repositioned. The magnetic field is measured at five vertical positions between the PPT electrodes (2.8 mm, 8.7 mm, 13.8 mm, 19.5 mm, and 23.4 mm from the cathode) and two axial positions away from the propellant face. In the axial position further away from the propellant face, the probe is positioned such that the Probe #1 is placed in the location Probe #3 occupied before the probe was moved back. Thus five axial locations are sampled (z=10.4 mm, 18.9 mm, 25.7 mm, 34.2 mm, and 41.0 mm) with two measurements at the z=25.7 mm location. The probe coil locations are measured from photographic images of the probe within the PPT electrodes to an accuracy of 0.1 mm.

A. Probe Perturbations

To characterize possible effects that the presence of the probe may have on the PPT discharge, images were collected of the plasma broadband emission with an intensified framing camera with a 10 nS gate time. In the images, shown in Fig. 4, the probe stem is clearly visible backlighted by the plasma emission. The characteristic V-shape of the discharge arc is observed in each image. The arc is observed to retain its basic shape regardless of the probe position suggesting that the probe is not affecting the discharge structure.

Aligning Probe #3 from the inner probe placement with the position of Probe #1 in the outer probe placement is done to examine probe effects on the magnetic field structure. With no perturbations, these probes should measure the same magnetic field. However if perturbations do occur, it would be expected that Probe #3 from the inner position would see a significant difference in magnetic field since it has 1.1 cm of additional cladding material in the upstream location available for ablation.

Figure 5 shows a comparison of the measurements for these locations with the probe placed at 8.3 mm from the cathode in the vertical direction. Each of the waveforms from Fig. 5 represents the average of 10 measurements with error bars calculated from the standard deviation of these measurements. The magnetic field measured in the two cases agrees within the measurement accuracy. Measurements at the other vertical location show similar agreement. This agreement suggests that probe perturbations are not affecting the magnetic field structure.

B. Magnetic Field Distribution

The PPT discharge current is shown in Fig. 6. The three waveforms in Fig. 6 correspond to the average current measured over 10 discharges and waveforms where the standard deviation has been added to and subtracted from the average. The discharge current is observed to be very reproducible with minimal deviations from the average.

The time variation of the PPT magnetic field for five axial locations is shown in Fig. 7. The waveforms are again the average of 10 discharges with the error bars calculated from the standard deviation. Comparison with Fig. 6 shows the PPT magnetic field structure to have significantly more shot-to-shot variation than the discharge current. The shot-to-shot variations are the dominant source of measurement uncertainty in the magnetic field measurements. The magnetic field peak from Fig. 7 clearly moves axially in time away from the propellant face suggestive of a current front propagating under the influence of the Lorentz force. Plotting the time and position of the magnetic field maxima, Fig. 8, shows a relatively constant velocity of 17 km/s. This is in relative agreement with the 20 – 25 km/s current-front velocity measured in the 100 J side-fed PPT.[11]

The magnetic field measurements from the 25 sampling locations are assembled into a 2-dimensional contour plot in Fig. 9 at 2 μS after the discharge initiation. The contour uses the average of 10 magnetic field measurements at each location. The cathode is at the bottom of the contours, the anode is at the top, and the propellant face is on the left (the vertical orientation is reversed from the images of Fig. 4). Also shown in Fig. 9 are the effects of the magnetic field measurement uncertainty on the contour structure where the standard deviation has been added (labeled "+SD") and subtracted ("-SD") from the average value. Although the magnitude of the field contours change, the general structure remains the same.

Figure 10 shows the magnetic field contours during the first ½-cycle of the discharge current. For the symmetric case, where there is no magnetic field vector component in the vertical and axial directions, the contours also represent lines of the plasma current. The plasma current front propagates away from the propellant face with a current channel width of approximately 1 cm that increases in time. Figure 10 is best viewed in contrast to Figure 11, which shows similar plots for the second half-cycle of the PPT current. In Fig.11 the current channel width is significantly greater, ranging from 2 to 3 cm Indicative of magnetic field predominantly diffusing into the plasma as opposed to driving magnetohydrodynamic motion.

IV. Discussion

The magnetic field contours suggest that during the first half cycle magnetohydrodynamic motion of the plasma and current channel occurs which enables the plasma to be efficiently accelerated to high velocities. The diffusion of the magnetic field into the plasma occurs on a time-scale slower than the propagation velocity. During the 2nd half-cycle, a lower energy discharge is applied to a cold partially ionized plasma. Instead of bulk

magnetohydrodynamic motion, the fields resistively diffuse into and possibly through the plasma. The magnetic field in the second ½ cycle thus primarily heats the plasma. Some of this energy will be converted to thrust in the subsequent thermal expansion of the heated plasma, although probably not as efficiently as the ideal case where the magnetic field magnetohydrodynamically accelerates the plasma with no heating. This observation of a propagating arc during the first ½-cycle followed by a stationary ablation arc in the second ½-cycle has been proposed theoretically by Turchi.[12] Measurements of two waves of plasma velocity in the PPT exhaust by Eckman at al. At NASA-LeRC were thought to be experimental evidence of this phenomenon.[13]

The PPT capacitor undergoes a 40% voltage reversal in the second ½ cycle of the discharge.[4] Thus, 84% of the energy delivered to the electrodes is dissipated in the first ½ cycle of the current. The 16% of the energy dissipated in the subsequent cycles heats the plasma creating minimal thrust. This energy will also be expected to cause additional propellant vaporization from the Teflon face. Since there is insufficient energy for electromagnetic acceleration, this represents a propellant loss mechanism as well as an energy loss mechanism. Several design options exist or have been proposed that may ameliorate this loss:

- Increasing the discharge energy so Lorentz acceleration can occur in the second ½ cycle,
- Crowbarring the capacitor after the current peak to continue the discharge without giving the plasma an opportunity to cool between cycles,
- Optimizing the PPT discharge frequency.

To accurately assess and interpret the implications of the magnetic field structure on the PPT performance requires similarly detailed measurements of other plasma properties. Foremost among these is the plasma density. Although interferometers have been successfully used to measure the plasma electron density[4.11] during the discharge, this diagnostic has generally been limited to single-point measurements and is also unable to measure neutral densities during the discharge. AFRL, in collaboration with the University of Illinois is presently developing a 2-color interferometer with a Herriott cell for path length multiplication. Design specifications indicate that this diagnostic may have the capability to simultaneously measure the electron and neutral densities throughout the PPT discharge.

A major point of this work is determining whether the magnetic fields can be accurately mapped out in the PPT without perturbing the plasma properties. Based on Figs. 4 and 5 the quartz-clad magnetic field coils appear to be successful in measuring the PPT magnetic field without perturbation. The main problem with the diagnostic is clearly the overly large measurement uncertainties. The dominant source of measurement uncertainty is the poor shot-to-shot reproducibility of the PPT discharge. This is evidenced by the high reproducibility of the total PPT current (Fig. 6) compared to the magnetic field strengths (Fig. 7). Although the PPT operation appears reproducible based on external diagnostics such as total current, the detailed structure of the discharge can change dramatically from shot to shot. The accuracy of the present measurements are sufficient to make qualitative conclusions concerning the physics of the PPT discharge, however the accuracy is probably insufficient for use in detailed numerical models of the PPT physics.

Two general options are available to increase the measurement accuracy of the 2-dimensional magnetic field structure. The first is to develop a 2-dimensional magnetic field diagnostic that can attain a snapshot of

the magnetic field structure on a single discharge. This generally requires a ground-state electronic transition that can be resonantly excited with a laser. No obvious candidate for such a diagnostic has been observed using emission spectroscopy, however options remain for adding a small amount of High-Z material with suitable transitions.

The second option is to improve the reproducibility of the PPT discharge. To this end, at AFRL a second-generation laboratory PPT, XPPT-1B has been developed and tested. The primary advantage of XPPT-1B, as it relates to the present work, is that only 1 sparkplug is used in the electrode. The design thus follows more closely to the EO-1 PPT design by Primex Aerospace, as opposed to XPPT-1 following the original LES 8/9 design. Performance tests of XPPT-1B show a mass ablation rate (~25 μg/discharge) and thrust (270 μN) at 20J approximately equivalent to the flight model PPTs indicating that it is a reasonable laboratory equivalent. Future tests will determine whether an increase in the reproducibility of the arc structure has also been achieved.

V. Summary and Conclusions

Magnetic field probe arrays are developed for use in the PPT which consist of 3 magnetic pickup coils encased in a quartz sheath. Measurements of the discharge arc structure and comparison of probe measurements at different locations indicate that the probes are non-perturbing to the PPT plasma. Measurement accuracy of the probes is limited by the poor shot-to-shot reproducibility of the PPT discharge itself.

Measurements of the magnetic field structure in a 20J PPT show a propagating current sheath indicative of electromagnetic acceleration during the first current ½-cycle. During the second ½-cycle the magnetic field is observed to diffuse rapidly into the plasma with no observable magnetohydrodynamic motion. Energy dissipated in the second ½ cycle is presumed to resistively heat the plasma. It can only be recovered by the small amount of thrust created through the thermal expansion of the heated plasma. Approximately 16% of the energy delivered to the PPT electrodes is dissipated after the first ½ cycle, and is regarded as a source of energy inefficiency in the device.

VI. Acknowledgements

This work is supported by the Air Force Office of Scientific Research under the direction of Mitat Birkan. The authors acknowledge the assistance of Scott Engelman in performing the magnetic field measurements. The magnetic field probe design was developed by Ross McAfee, USAF. Frank Gulczinski assisted in the design and characterization of the calibration strip-line.

---

[1] W. J. Guman and D. M. Nathanson, "Pulsed Plasma Microthruster for Synchronous Orbit Satellite," J. Spacecraft and Rockets **7**, 409 (1970).

[2] Y. Brill, A. Eisner, and L. Osborn, "The Flight Application of a Pulsed Plasma Microthruster; the NOVA Satellite," AIAA/JSASS/DGLR 16th International Electric Propulsion Conference, AIAA Paper 82-1956, New Orleans, LA, Nov. 17-19, 1982.

[3] W. J. Guman and T. E. Williams, "Pulsed Plasma Microthruster for Synchronous Meteorological Satellite (SMS)," AIAA 10th Electric Propulsion Conference, AIAA Paper 73-1066, Lake Tahoe, NV, Oct 31 - Nov 2, 1973.

[4] Spanjers, G. G., McFall, K. A., Gulczinski, F. S., Spores, R. A., "Investigation of Propellant Inefficiencies in a Pulsed

Plasma Thruster," AIAA Paper 96-2723, July 1996.

[5] Gregory G. Spanjers, Jason A. Lotspeich, Keith A. McFall, Ronald A. Spores, "Propellant inefficiency resulting from particulate emission in a Pulsed Plasma Thruster," Journal of Propulsion and Power, Vol. 14, No. 3, May-June 1998.

[6] Gregory G. Spanjers, Jamie B. Malak, Robert J. Leiweke, and Ronald A. Spores, "The effect of propellant temperature on efficiency in a pulsed plasma thruster," Journal of Propulsion and Power, Vol. 14, No. 4, July-August 1998.

[7] Vondra, R. J., and Thomasson, K. I., "Performance Improvements in Solid Fuel Microthrusters," *J. Spacecraft*, Vol. 9, 1972, p. 738.

[8] Lynn Arrington et al., "A Performance Comparison of Pulsed Plasma thruster Electrode Configurations," IEOPC 97-127, 25th Intl. Electric Propulsion Conference, Aug. 1997.

[9] D. E. T. F. Ashby, "A Simple Theory of Wall Evaporation in a Pulsed Gas Discharge," Plasma Physics (J. of Nuclear Energy Part C), Vol. 5, pp. 83-87, 1963.

[10] R. H. Lovberg, in Plasma Diagnostics, K. Huddlestone ed., (Academic Press, NY, 1968).

[11] Antropov et al., "Parameters of Plasmoids injected by PPT," AIAA Paper 97-2921, 33rd Joint Propulsion Conference, Seattle, WA, July 1997.

[12] P. J. Turchi, P. G. Mikellides, "Modeling of ablation-fed Pulsed Plasma Thrusters," AIAA 95-2915, 1995.

[13] R. Eckman et al., "Experimental investigation of the LES 8/9 Pulsed Plasma Thruster," IEPC Paper 97-126, 25th Intl Electric Propulsion Conference, Aug. 1997.

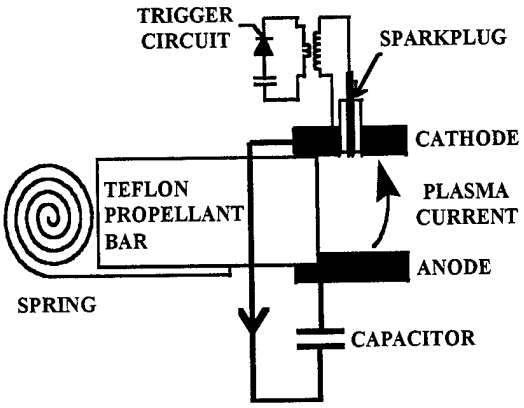

Fig. 1 Schematic diagram of a Pulsed Plasma Thruster

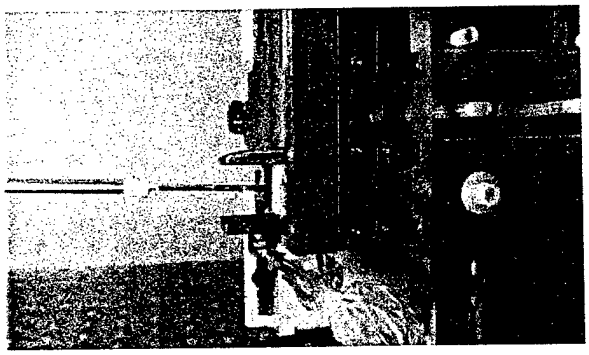

Fig. 2 Magnetic Probe Array inserted into Pulsed Plasma Thruster XPPT-1

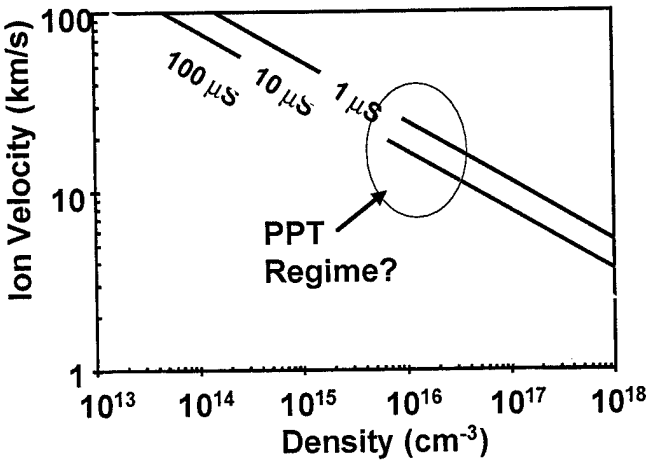

Fig. 3 Boil time as a function of ion velocity and density for a Quartz cladding

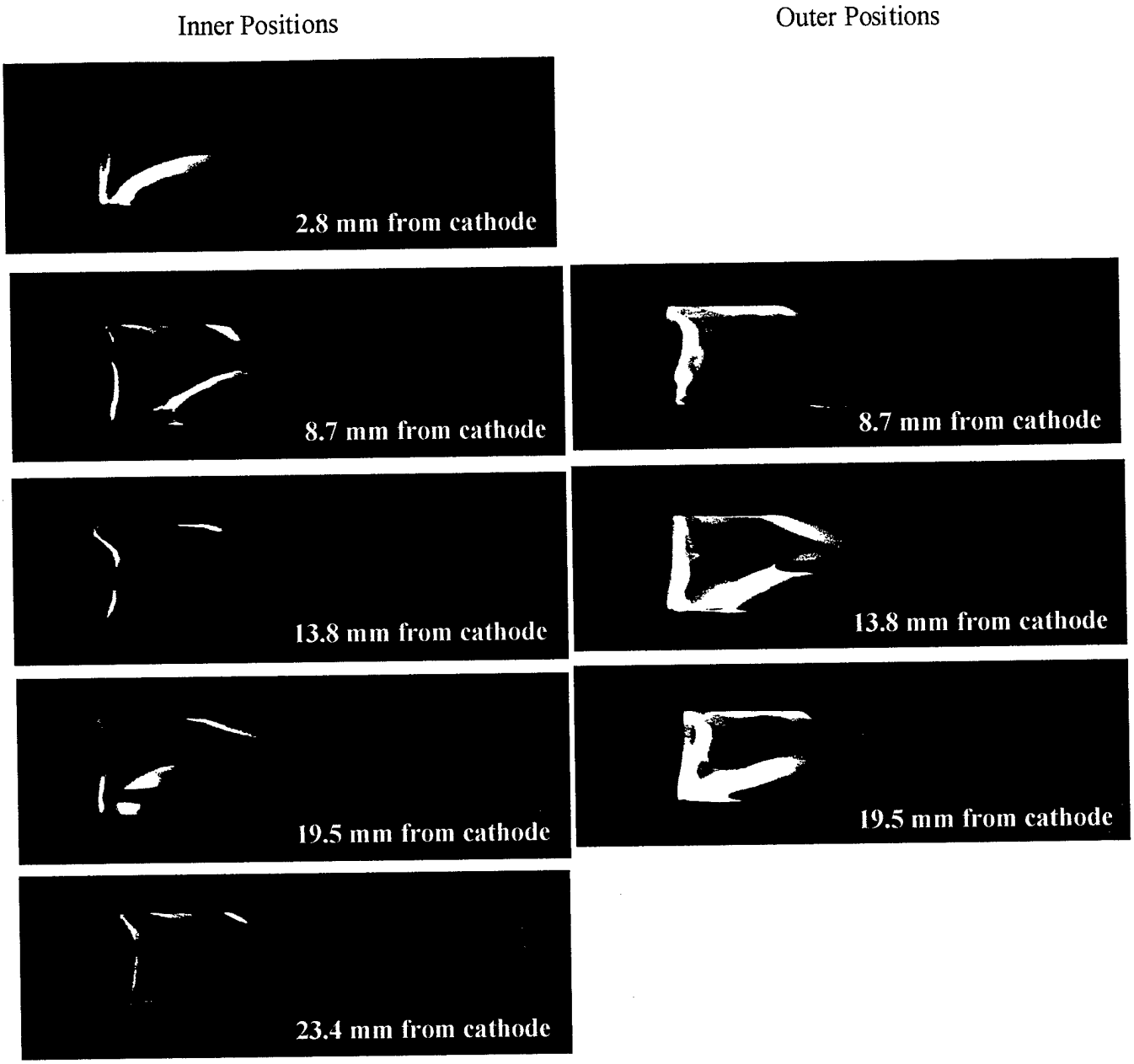

Fig. 4 Intensified broadband emission images of the PPT discharge arc with the probe inserted at varied locations

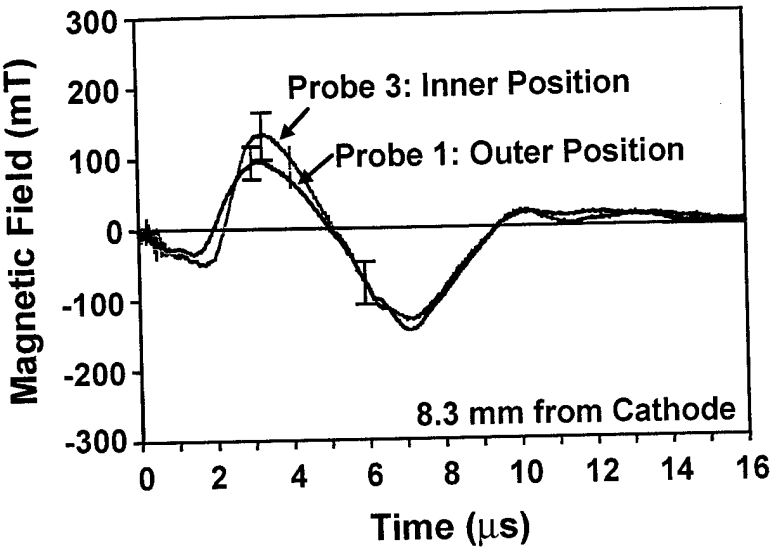

Fig. 5 Magnetic fields measured 8.3 mm from the cathode and 25.7 mm from the propellant face using 2 different magnetic field probes.

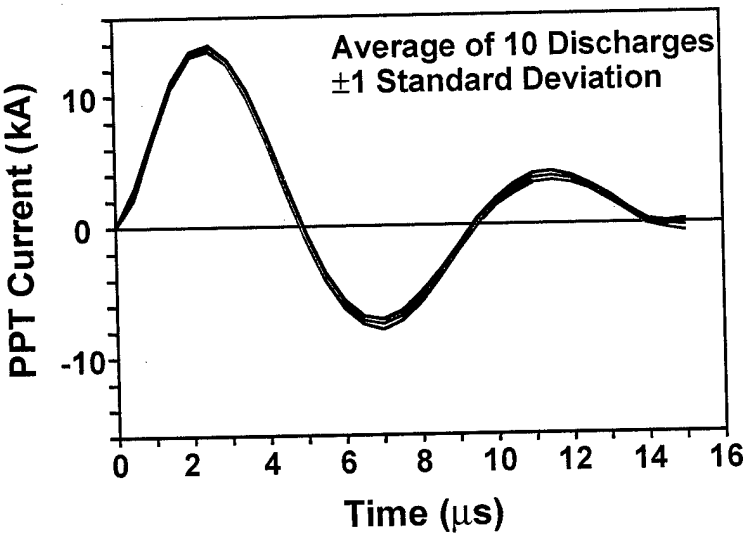

Fig. 6 PPT discharge current. The three waveforms correspond to the average of 10 discharges and the standard deviations.

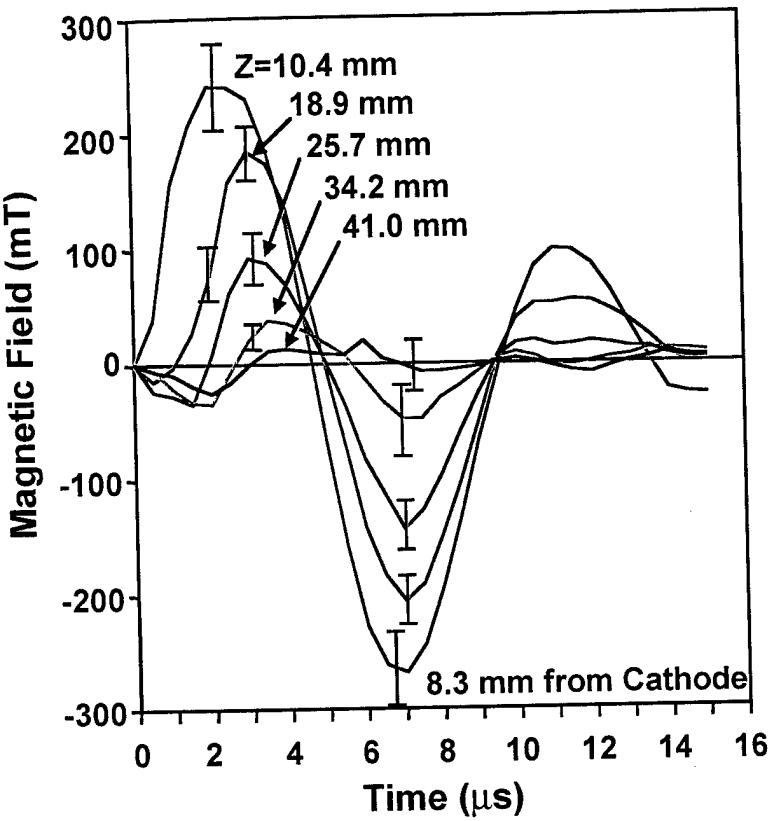

Fig. 7 Magnetic fields measured 8.3 mm from the cathode and at several distances from the propellant face.

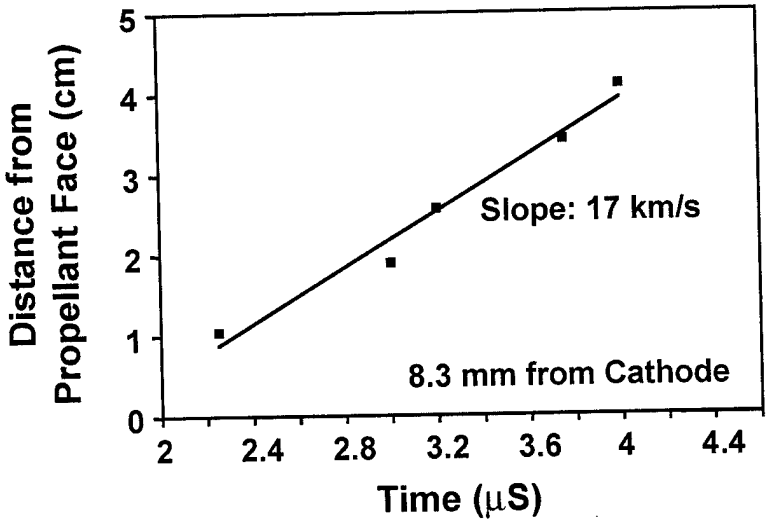

Fig. 8 Propagation of the peak magnetic field 8.3 mm from the cathode

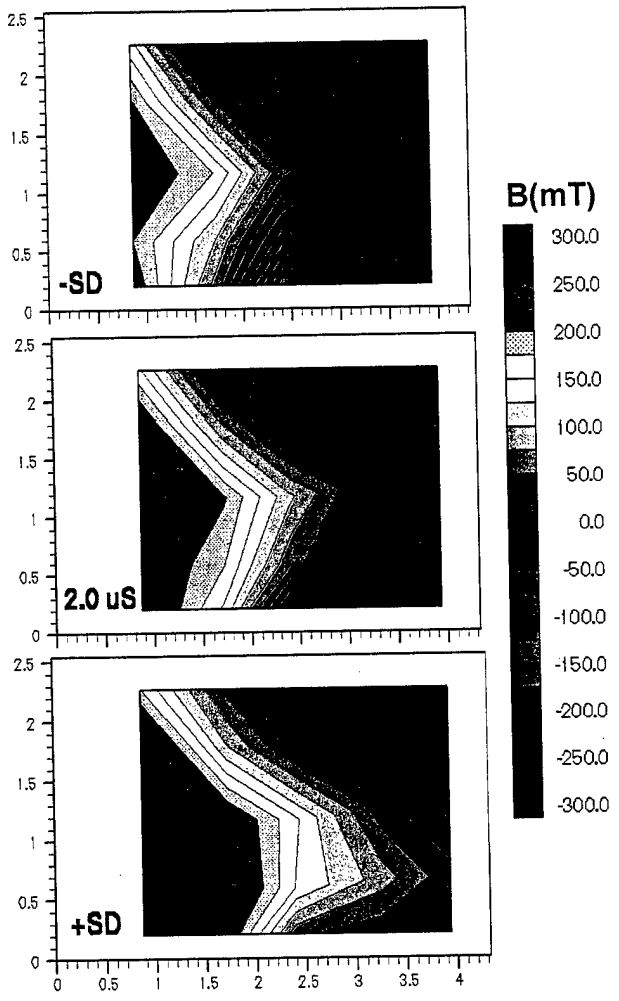

Fig.9 The effect of measurement uncertainty on the magnetic field contour calculations. The center plot uses the average of 10 magnetic field measurements for each of the 25 locations at 2 μS. The upper and lower contours use the same data with the standard deviation subtracted from and added to the average respectively.

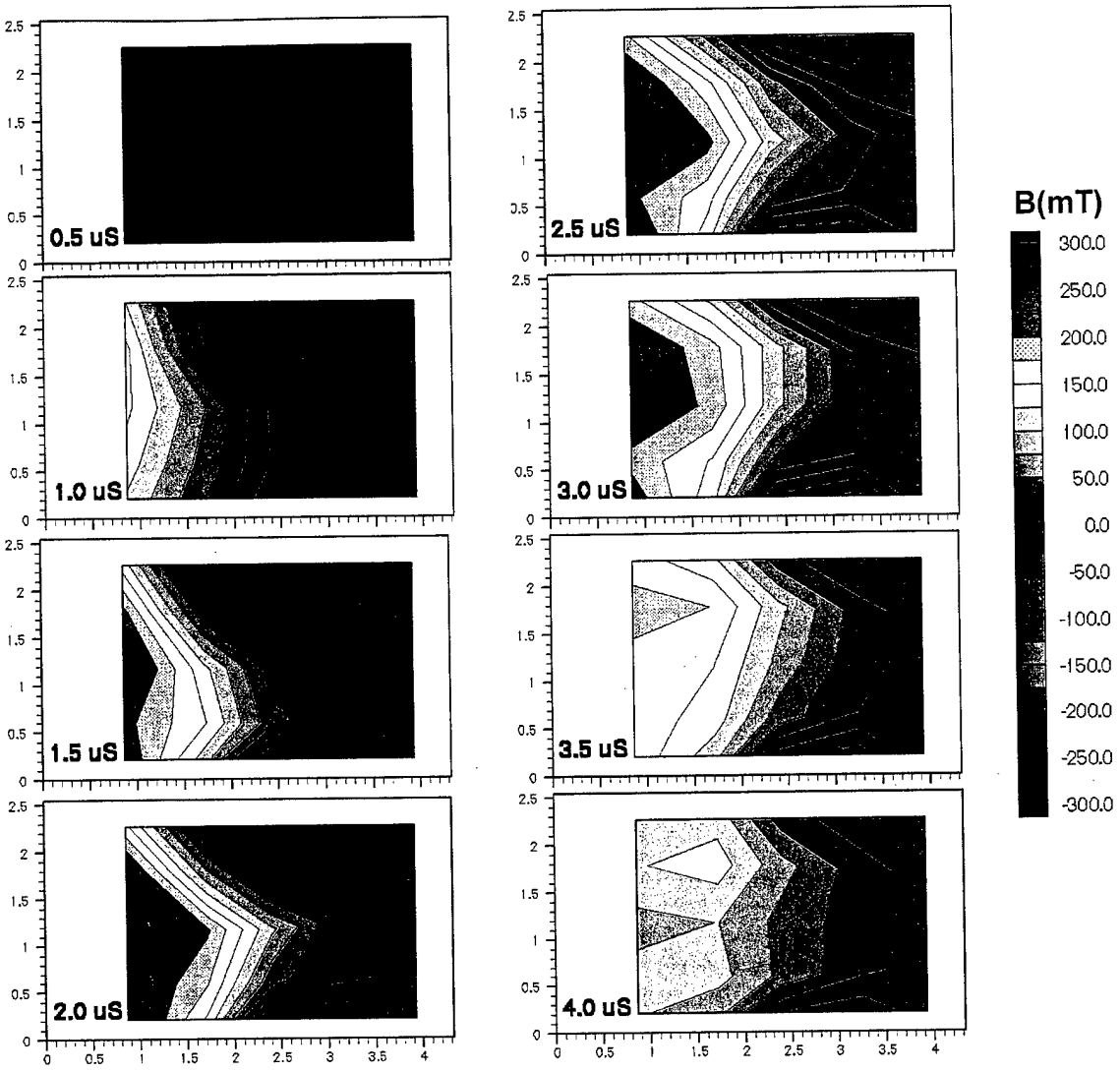

Fig. 10 Magnetic field contours during the first 1/2-cycle of the PPT discharge current. Dashed contours correspond to negative values.

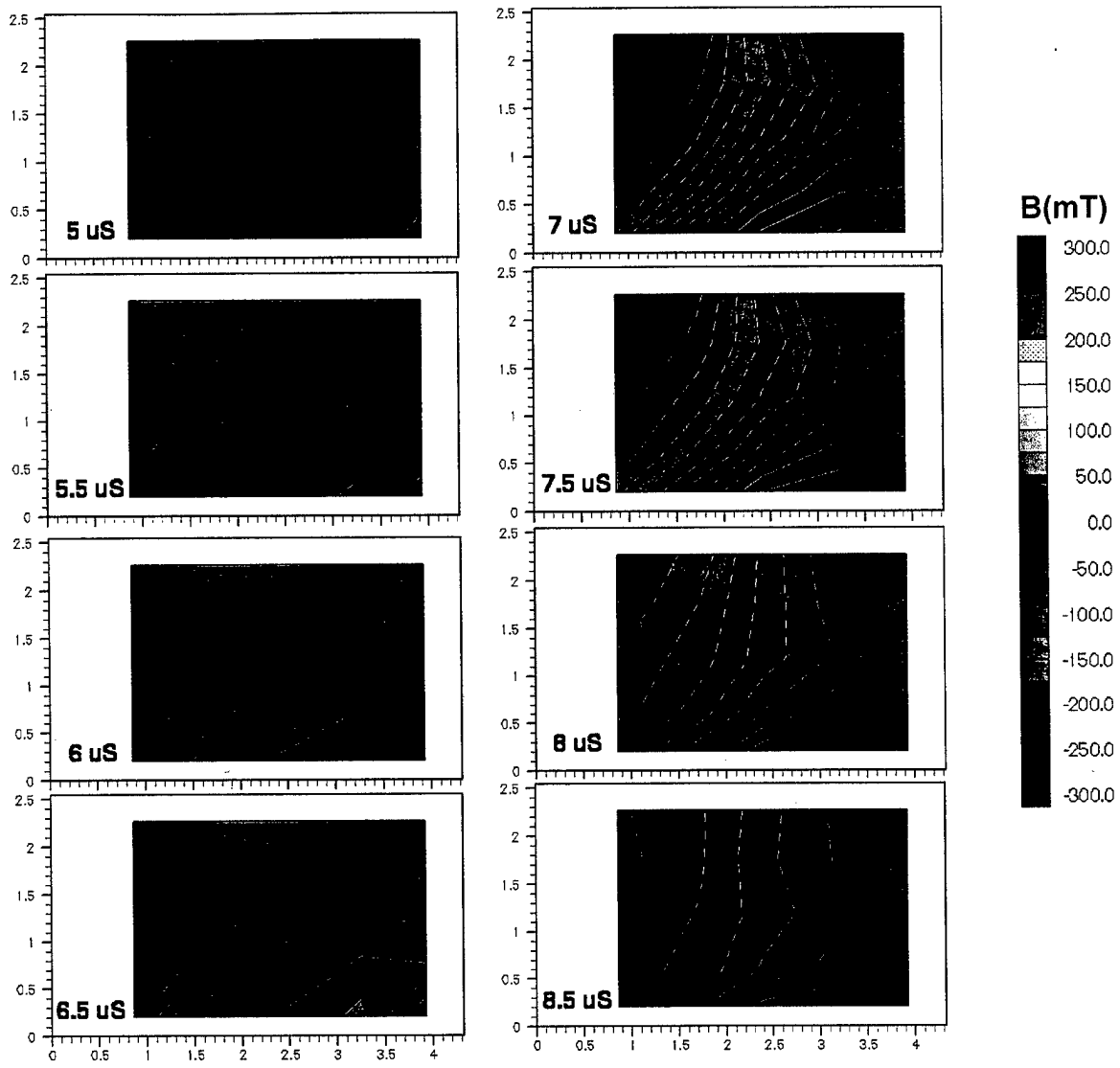

Fig. 11 Magnetic field contours during the second 1/2-cycle of the PPT discharge current.